Austral Summer Sea Ice Melt Revealed in Antarctic ERS-1/2 and NSCAT Scatterometer Data

Mark R. Drinkwater and Xiang Liu
Jet Propulsion Laboratory,
California Institute of Technology,
4800 Oak Grove Drive, Pasadena, CA 91109
Tel: +001 (818) 354 8189
Email: m.drinkwater@jpl.nasa.gov
URL: http://oceans-www.jpl.nasa.gov/polar

Introduction

The first *in-situ* field observations of Antarctic austral summer sea-ice melt were made in the Bellingshausen Sea by Arctowski (1908) on *Belgica* in 1899, and later by Wordie (1921) during the ill-fated drift of *Endurance* in the Weddell Sea from 1914-1916. It has been 100 years since these pioneering ship drift experiments, yet little more is known about the spatial extent, duration, frequency of seasonal surface melting of sea ice during the austral summer (December through March), or indeed its interannual variability. Both experimenters independently reported that Antarctic sea ice does not experience widespread vigorous summer surface melting, as is characterized by the formation of extensive ponding at melt maximum in the Arctic (Gogineni *et al.*, 1992). Despite surrounded by relatively warm ocean surface waters, some energy balance studies have suggested that the resulting combined surface radiative and turbulent heat fluxes are insufficient to induce widespread, protracted surface melting (Andreas and Ackley, 1982).

The so-called "albedo-feedback" effect (Curry *et al.*, 1995) results in Arctic melt ponding and ultimate removal of a large fraction of sea-ice during the summer months. This feedback operates when snow surface melting reduces the mean spectral albedo of the surface from ~0.9 to 0.7 or less (via thermal alteration of snow grains and reduced reflectivity, and appearance of water in liquid phase) (Maykut, 1985). Increased absorption of short wave and trapped long-wave radiation results in larger amounts of energy expended in melting of the snow and sea ice cover and a further reduction in the spectral albedo. This positive feedback causes a vicious cycle which accelerates the removal of large expanses of Arctic ice too thin to survive an extended summer period of combined surface, lateral and bottom melt. In Antarctica, the sea ice is completely surrounded at lower latitudes by ocean. Intuitively, therefore, summer storms are expected to be capable of delivering significant quantities of heat to the austral summer ice pack. Yet large regions of sea ice manage to survive the austral summer in spite of this and the relatively high ocean heat flux environment (McPhee and Martinson, 1994; Martinson and Iannuzi, 1998).

Scatterometer Melt Observations

This study attempts to answer questions regarding austral summer surface melting using microwave radar images of Antarctic sea ice generated from wind scatterometer measurement data. Two independent radar image time-series were created using C-band ERS-1/2 Wind Scatterometer (hereafter ESCAT) data delivered by IFREMER (Drinkwater and Long, 1993), and Ku-band NASA Scatterometer (NSCAT) data (Long and Drinkwater, 1999). ERS-1/2 images from the period 1992 until 1997 are exploited to study seasonal to interannual variability in surface melting. Comparative simultaneous NSCAT images are available for the 1996 - 1997 austral summer melt season.

Microwave radar image backscatter coefficient data, σ^{o}_{vv} (normalised to 40° incidence angle) are particularly sensitive to the appearance of liquid water in the snowpack at the time melting begins. Arctic examples demonstrate the sensitivity of σ^{o}_{vv} (hereafter A) to the effects of snow and ice surface melt (Drinkwater and Carsey, 1991; Gogineni *et al.*, 1992; and Winebrenner *et al.*, 1994). Although 3-daily ESCAT or NSCAT A images have relatively coarse resolution > 10 km (in contrast to 30m resolution 100 x 100 km ERS-1/2 Synthetic

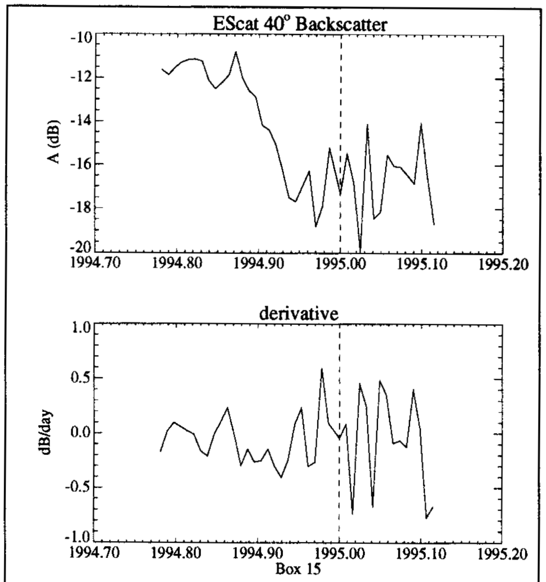

Figure 1 Melt onset in the north-west Weddell Sea (64°S 56°W) in 1994, expressed as; (a) mean A values (σ^{o}_{vv}) at 3-day intervals; and (b) their time derivative. Vertical dashed line indicates the beginning of the 1995 calendar year.

Aperture Radar) images, the scatterometer provides an efficient, sensitive means of detecting widespread surface melting over the entire sea-ice cover at 3-day intervals.

Recently, Drinkwater *et al.* (1998) demonstrated that Antarctic ESCAT images exhibit similar characteristics over melting ice as radar data from the Arctic summer ice cover. The onset of melting is characterized in Fig. 1 by an abrupt decline in backscatter of –3 dB or more, over a contiguous time period of several days. The top panel in Fig. 1 indicates a reduction in backscatter of approximately 7 dB over 21 days (*i.e.* seven consecutive images at 3-day intervals) in the region observed to be melting in the summer of 1994 - 1995. The accompanying data shown in the lower panel of Fig. 1 indicate that the time derivative $\delta A/\delta t$ remains negative for a period of around 8 consecutive images (or 24 days) during this initial melt onset period. The combination of these two criteria has the advantage of filtering out small rapid fluctuations resulting from mid-winter storms or oscillating air temperatures. Melt-freeze cycles are also captured by negative and positive swings, respectively, in the derivative time-series. Positive derivative values (cooling phases) are later rejected during calculation of the number of cumulative melt days experienced throughout the contiguous austral summer season.

Melt Detection

A melt-detection algorithm has been developed for general application to ESCAT or NSCAT scatterometer images resampled to equal pixel spacing (8.8 km). Images are first smoothed with a two-dimensional Gaussian filter (with ~ 56 km half-width) and backscatter values stored in a stack of seven consecutive images (*i.e.* 21-day window) starting from an arbitrary date in early November (prior to melt onset). Then the algorithm is successively applied to each pixel within the sea-ice region (presently predefined as the pixels falling between SSM/I ice edge location and the coast of Antarctica). After each ice-covered pixel is searched and checked for melting, a new image is loaded and the process restarted.

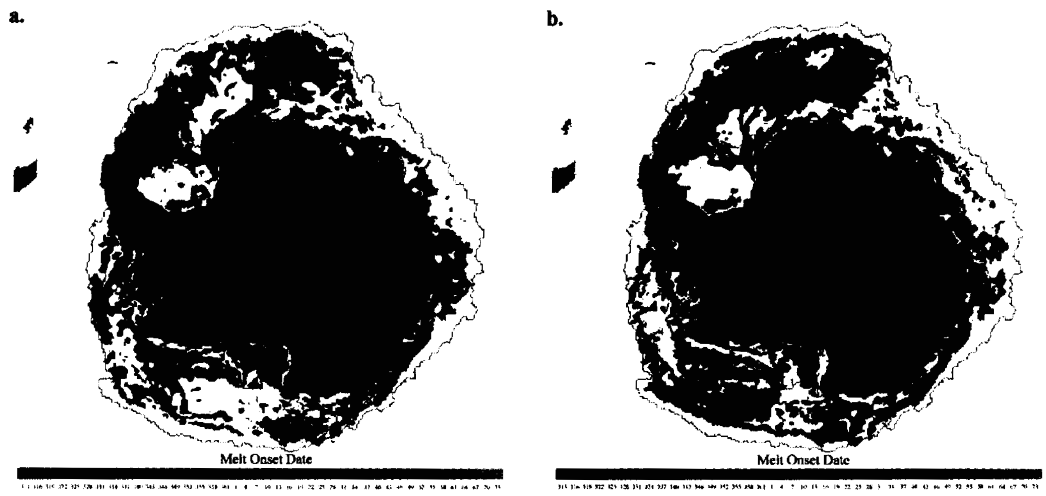

Figure 2 Detection of Melt Onset in (a) ERS-2 (b) NSCAT data for the 1996-97 austral summer season.

Onset of melt is recorded as the date after which several significant, consecutive reductions in backscatter are detected, each pixel requiring a combination of threshold criteria to be met. In the case of Antarctic sea ice these criteria require that the first and second images after melt onset have individual pixel value decreases exceeding -0.5 dB, and that the total decrease exceeds –3 dB over an adjustable time period exceeding 2 images (> 6 days). When applied to the pixel values plotted in Fig. 1., melt onset is automatically selected as day 319 (1994.874) or 15 November. Fig. 2 shows composite results from both satellite instruments for the austral summer of 1996 - 1997, each recovered using the automated melt detection algorithm. The coloured bar and legend indicate the day of year on which melting began. Blue and greens indicate melt onset during November and December, while brown, red, orange and yellows highlight successively later melt onset during January, February or

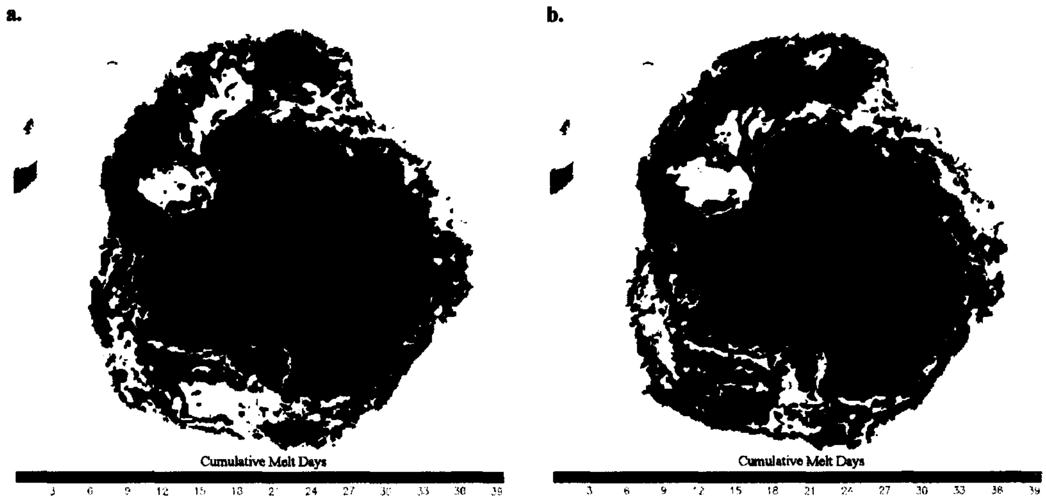

Figure 3 Cumulative surface melt days detected by (a) ERS-2; and (b) NSCAT data in the 1996-97 austral summer season.

March, respectively. The initial outer ice margin location is indicated for day 313 (8 November) at the beginning of ice edge recession, prior to melt onset. An inner line delineates the ice extent at the end of the run (day 73: 14 March).

Cumulative melt days throughout the summer season are also recorded from the melt onset date forwards. Since fluctuations in *A* values are common, periods of positive time derivatives are rejected. Fig. 3 shows the comparative results for number of cumulative melt days from both satellite instruments. Notably, in order to obtain similar results for C- and Ku-band frequencies, the melt criteria had to be significantly relaxed (from –3 dB to –1 dB drop) for ESCAT data. This is partially attributable to increased noise, reduced resolution, and lower sensitivity of the C-band *A* values to the appearance of moisture in the snow (*i.e.* reduced dynamic range).

Conclusions

Preliminary results indicate that both ERS-1/2 (C-band) and NSCAT (Ku-band) scatterometer images may be used effectively to monitor the large-scale surface characteristics of austral summer ice in Antarctica. Since the value of radar backscatter coefficient at 40° incidence is sensitive to changes in reflectivity, surface melting has a large impact on the *A* values, typically exceeding -3 dB reduction. Though the response to snow surface melting is basically the same as that recorded in the Arctic (since it is independent of the ice type), these preliminary results show that Antarctic ice responds quite differently from its Arctic counterpart during the summer season. Cumulative melt days recorded by both instruments confirm that austral summer melting is short-lived, patchy and ephemeral. The only locations experiencing protracted vigorous melting (exceeding 30 days) in 1996-97 were regions bordering the Antarctic peninsula, in the Weddell and Bellingshausen Seas, and East

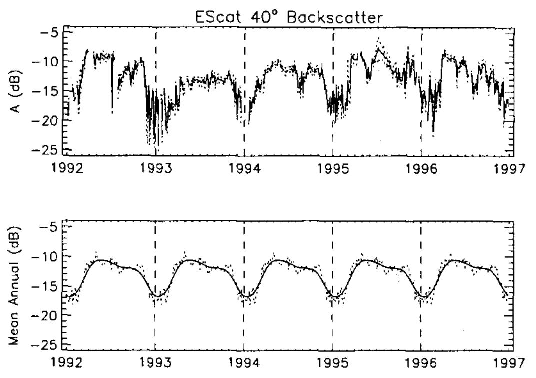

Figure 4 Interannual time series from the northwest Weddell Sea (64°S 56°W) indicating (a) A values; and (b) the mean seasonal cycle.

Antarctic coastal regions. The southernmost melting region is observed in the Ross Sea, while the interesting point location located in the Amundsen Sea is discovered to correspond with the location of the large drifting Thwaites iceberg (A-10).

The primary conclusion from this work is that atmospherically led austral summer surface melting is far less extensive in time or space than that experienced in the Arctic. Melt onset patterns do not appear to occur in a spatially coherent manner, nor as rapidly as was observed in the Beaufort Sea by Winebrenner *et al.* (1998). Melt onset dates in Fig. 2 do, however, indicate a poleward propagating melt front, moving progressively southwards as air temperatures increase. Although rapidly moving storms bring enough heat to cause temporary surface melting, the scatterometer image record conclusively shows that protracted summer surface melting in a specific region is rare and more likely short-lived. Instead of long periods with depressed backscatter coefficients, the summer is characterized by large fluctuations in backscatter indicating melting and freezing cycles. This behaviour is not unique to the sea ice, but is also observed on neighbouring ice shelves, where meteorological station data confirm the amplitude of the temperature fluctuations (Drinkwater *et al.*, 1998).

The retreat of the Antarctic summer ice margin appears not to be led by the atmosphere, but rather by a balance between ocean heat flux and sea-ice dynamics. Although melt onset is detected in mid-November over large areas of the outer Antarctic ice margin, the negligible number of cumulative melt days (in these regions) implies instead that ice-drift regulated mass flux at the ice margin balances largely ocean heat flux-induced melting. Interannual time series such as that shown in Fig. 4 (after Drinkwater *et al.*, 1998) imply that there is significant interannual variability in the dynamically-regulated component of this balance. In this way smaller rates of northwards advection contribute to more rapid ice edge recession, yet also survival of larger fractions of perennial ice in the southern Weddell Sea and Amundsen basin.

Our future work involves a long-term consistent analysis of these data by applying the melt algorithm over the span of 6 years between 1992 and 1998. Results of this analysis will enable us to draw conclusions regarding the interannual variability in atmospherically-led surface melting over the contiguous period of ERS-1 and ERS-2 data reception. These results will be published in a future Special Scatterometer Issue of the Transactions of Geoscience and Remote Sensing.

Acknowledgements

These data were delivered by ESA under Project AO2.USA.119. Doug Low is acknowledged for his important contribution to the analysis of the ERS Wind Scatterometer data. MRD and XL completed this work at Jet Propulsion Laboratory, California Institute of Technology under contract to the National Aeronautics and Space Administration and funded by Dr. Prasad Gogineni of NASA Code YS.

References

Andreas, E. L., and Ackley, S. F., On the differences in Ablation Seasons of Arctic and Antarctic Sea Ice, *Journal Atmospheric Science*, 39, 440-447, 1982.

Arctowski, H., Les Glaces: glace de mer et banquises. Resultats du Voyage du S.Y. Belgica en 1897-1898-1899, *Rapports Scientifiques*, Vol. 5., J.E. Buschmann, Antwerp, [Trans., NTIS AD 881 363], 3-55, 1908.

Curry, J.D., J.L. Schramm, E.E. Ebert, Sea Ice-Albedo Climate Feedback Mechanism, *J. Climate*, 8, 240-247, 1995.

Drinkwater, M.R., Satellite Microwave Radar Observations of Antarctic Sea Ice. In C. Tsatsoulis and R. Kwok (Eds.), *Analysis of SAR Data of the Polar Oceans*, Chapt. 8, 147-187, Springer-Verlag, Berlin, 1998a.

Drinkwater, M.R., Active Microwave Remote Sensing Observations of Weddell Sea Ice. In M.O. Jeffries (Ed.) Antarctic Sea Ice: Physical Processes, Interactions and Variability, *Antarctic Research Series*, 74, 187-212, American Geophysical Union, Washington, D.C., 1998b.

Drinkwater, M.R., and F.D. Carsey, Observations of the late-summer to fall transition with the 14.6 GHz SEASAT scatterometer, *Proc. IGARSS '91 Symposium*, Vol. 3, IEEE Catalog #CH2971-0, June 3-6, 1991, Espoo, Finland, 1597-1600, 1991.

Drinkwater, M.R., D.G. Long, and D.S. Early, Enhanced Resolution Scatterometer Imaging of Southern Ocean Sea Ice, *ESA Journal*, 17, 307-322, 1993.

Drinkwater, M.R., X. Liu, D. Low, and P. Wadhams, Interannual Variability in Weddell Sea Ice from ERS Wind Scatterometer, *ESA SP*, 424, 1999.

Drinkwater, M.R., X. Liu, and D. Low, Interannual Variability in Weddell Sea Ice from ERS Wind Scatterometer, *Proc. IGARSS '98*, Seattle, Washington, 6-10 July, 1998., IEEE Catalog # 98CH36174, Vol. 4, 1982-1984, 1998.

Gogineni, S.P., R.K. Moore, T.C. Grenfell, D.G. Barber, S. Digby, and M.R. Drinkwater, The Effects of Freeze-up and Melt Processes on Microwave Signatures, In *Microwave Remote Sensing of Sea Ice*, (Ed.) F.D. Carsey, American Geophysical Union, Geophysical Monograph 28, Chapter 17, 329-341, 1992.

Long, D.G., and M.R. Drinkwater, Cryosphere Applications of NSCAT Data, *IEEE Trans. Geosci. and Remote Sens.*, In Press.

Low, D., The Validation of ERS-1 Summer SAR Data for Antarctic Summer Sea Ice, *Unpublished M. Sc. Thesis*, 143pp., 1995.

Martinson, D.G., and R.A. Iannuzzi, Antarctic ocean-ice interaction: implications from ocean bulk property distributions in the Weddell Gyre. In M.O. Jeffries (Ed.) Antarctic Sea Ice: Physical Processes, Interactions and Variability, *Antarctic Research Series.*, 74, 243-271, American Geophysical Union, Washington, D.C., 1998.

Maykut, G.A., The Surface Heat and Mass Balance, In The Geophysics of Sea Ice, (Ed.) N. Untersteiner, 395-463, Plenum, New York, 1985.

Winebrenner, D.P., E.D. Nelson, and R. Colony, Observations of melt onset on multiyear Arctic sea ice using the ERS 1 synthetic aperture radar, *J. Geophys. Res.*, 99, 11, 2225-22441, 1994.

Winebrenner, D.P., D.G. Long, and B. Holt, Mapping the Progression of Melt Onset and Freeze-up on Arctic Sea Ice using SAR and Scatterometry. In C. Tsatsoulis and R. Kwok (Eds.), *Analysis of SAR Data of the Polar Oceans*, Chapt. 7, 129-144, Springer-Verlag, Berlin, 1998.

Wordie, J.M., Shackleton Antarctic Expedition, 1914-1917: The natural history of pack ice as observed in the Weddell Sea, *Trans. Roy. Soc. Edinburgh*, 52, 795-829, 1921.